Pulsed heating atomic layer deposition (PH-ALD) for epitaxial growth of zinc oxide thin films on c-plane sapphire

Journal:	*Dalton Transactions*
Manuscript ID	DT-ART-10-2021-003581.R1
Article Type:	Paper
Date Submitted by the Author:	28-Nov-2021
Complete List of Authors:	Piercy, Brandon; Georgia Institute of Technology, Material Science and Engineering Wooding, Jamie; Georgia Institute of Technology, Material Science and Engineering Gregory, Shawn; Georgia Institute of Technology, Materials Science and Engineering Losego, Mark; Georgia Institute of Technology School of Materials Science and Engineering

PULSED HEATING ATOMIC LAYER DEPOSITION (PH-ALD) FOR EPITAXIAL GROWTH OF ZINC OXIDE THIN FILMS ON C-PLANE SAPPHIRE

Brandon D. Piercy,[1] Jamie P. Wooding,[1] Shawn A. Gregory,[1] Mark D. Losego[1]

[1]School of Materials Science and Engineering, Georgia Institute of Technology, Atlanta, GA

Abstract

An *in situ* pulsed heating atomic layer deposition (PH-ALD) technique is used to grow heteroepitaxial ZnO thin films on c-plane sapphire from temperature-sensitive metalorganic precursors. During metalorganic precursor delivery, the substrate is maintained at a base temperature of 110 ˚C to prevent thermal decomposition of the precursors. After the substrate is sequentially exposed to the metalorganic precursor and water co-reactant at this low temperature, a high-power resistive heater is used to rapidly heat the substrate to between 400 and 900 ˚C to drive film crystallization. These *in situ* heat pulses enable epitaxial growth of (0001) ZnO films on c-plane sapphire. Rocking curves with FWHM of values as low as 0.53˚ are achieved. In contrast, films deposited entirely at 110 °C appear random polycrystalline and post-deposition annealing to 900 °C achieves only partial "epitaxial character" with a notably different in-plane orientation. Variations in heat pulse temperature and the number of deposition cycles between heat pulses are explored. Epitaxial growth persists up to 5 deposition cycles per heat pulse, with the 2θ-ω FWHM increasing to 1-2˚. To further reduce process times, a templating approach is also explored in which a limited number of "template" layers are initially deposited with PH-ALD followed by low-temperature ALD at 110 °C. Epitaxial growth is encouraged with as few as 5 cycles of PH-ALD followed by 495 cycles of low-temperature ALD. Crystal quality further improves by using up to 50 template cycles, with a 2θ-ω FWHM of

1.3˚. Epilayers also show enhanced photoluminescence (PL) at room temperature. These results demonstrate how *in situ* pulse-heating can be used to promote epitaxial film growth in ALD processes using temperature-sensitive metalorganic precursors.

1. Introduction

Atomic layer deposition (ALD) is a common processing technology for microelectronics manufacturing that is capable of depositing thin films with a high degree of thickness control and conformality.[1] A key characteristic of ALD is the use of sequential, self-limiting, complementary reactions to grow films in a step-wise manner. In conventional isothermal ALD processes, the phase and density of the final film are primarily determined by the precursor selection and the deposition temperature.[2] Since the "ALD window,"[3] defined as the temperature window where ALD-mode growth proceeds, is narrow for many precursors, controlling film structure often requires post-deposition annealing (PDA). However, PDA operates by bulk diffusion processes and does not exploit the intrinsic layer-by-layer growth of ALD. Other thin film growth techniques, particularly MBE, MOCVD, and PLD operate at growth temperatures exceeding 600 °C, which enables registration of the newly deposited layer to the underlying structure. Herein, we examine the use of short heat pulses after each ALD cycle to drive surface diffusion processes to encourage registration to the underlying crystalline structure. We term this process "pulsed-heating" ALD (PH-ALD).

The concept of using "heat pulses" during an ALD process has been previously reported for a limited number of material systems. Conley *et. al.*[4-5] and Nabatame *et. al.*[6] have examined the use of pulsed heating in the ALD deposition of HfO_x and $HfAlO_x$ films. When compared to ALD with post-deposition annealing, these researchers showed that *in situ* rapid thermal lamp anneals lowered dielectric leakage currents and increased film density. Langston *et. al.* examined *in situ* annealing during ALD of TiO_2 films and found that pulsed heating could drive the formation of a nanocrystalline structure.[7] These researchers used a method called flash-lamp annealing (FLA) ALD, where a high-powered xenon flash lamp irradiates the surface of a growing film between each ALD cycle. Henke *et. al.* also used FLA to densify a growing ALD Al_2O_3 film. These researchers found that *in situ* annealing increased film density by 10%, a value that could not be achieved with a 600 °C PDA alone.[8] However, to our knowledge, no reports exist in the open literature for using pulsed heating in an ALD process to drive epitaxial growth of a thin film.

One challenge of prior PH-ALD systems is the added engineering complexity required to integrate high power heating into an ALD reactor. In this work, we implement a simpler PH-ALD system designed around a small, high-power resistive heating element to alternate between a conventional isothermal ALD cycle and a heat pulse. To validate this system, we explore heteroepitaxial growth of ZnO on a c-plane sapphire (Al_2O_3) template. We choose this as a model system because epitaxial growth of ZnO is well-studied and reported in the open literature.

ZnO is a well-established material with applications in solar energy, photocatalysis, and piezoelectricity[9-11] and has been grown epitaxially with a number of techniques, including PLD[12], MBE[13-16], PED[17], MOVPE[18] and MOCVD[19]. Unlike most other ALD-grown films, ZnO is typically crystalline as deposited,[2] growing in the wurtzite phase. Prior work on hydrothermally-grown ZnO nanowires has shown that ALD ZnO can grow homoepitaxially on a ZnO seed layer.[20] Recently, Elam *et. al.*[21] demonstrated high quality ALD homoepitaxial growth of ZnO using standard diethylzinc and water precursors at deposition temperatures of 120-200˚C, which was attributed to the slow, layer-by-layer growth process intrinsic to ALD. ZnO has also been grown heteroepitaxially using ALD on substrates with different lattice mismatches - SiC[22] (6%), GaN[23-26] (1.8%), and c-sapphire (18.4%).[27-29] However, these prior heteroepitaxy systems were grown via high temperature, isothermal ALD using temperature-stable inorganic precursors. One study from Yang *et. al.* reported the grow of epitaxial ZnO on c-plane sapphire at 200 °C and observed improving crystallinity with post-deposition anneals up to 800 °C.[30] As such, being able to access similar heteroepitaxial systems with conventional, industrial metalorganic precursors, such as diethylzinc (DEZ), expands the potential for ALD as an epitaxial growth technique. In this report, we describe the first use of PH-ALD to grow ZnO heteroepitaxially on c-sapphire and show how the process can be used for templating to enable follow-on homoepitaxial growth.

2. Experimental

2.1 Deposition Conditions

PH-ALD deposition was conducted in a specialized home-built PH-ALD reactor with a custom Go software modeled after an existing LabVIEW code.[31] The reactor used a conventional hot-wall reactor design using a stainless steel cross as the reaction zone (Figure 1a). Nitrogen (99.999% purity, Airgas) was used as the carrier gas at a constant flow rate of 60 sccm, resulting in a chamber pressure of 1.7 Torr. For all PH-ALD processing, the chamber and all process lines were maintained at a constant temperature of 110 ˚C. An AlN/W high-power heater (Oasis Materials) with an area of 1 cm^2 was attached to copper wiring through an electrical feedthrough. Sapphire substrates were attached to the heater and temperature was measured with a type-K thermocouple using a stainless steel clip. Power was supplied to the heater using an external linear power supply set to constant current mode (B&K Precision). Figure 1b presents images taken through the chamber cross view port of a substrate during the heating and cooling phases of a heat pulse after a deposition cycle. ESI Figure 1 reports characteristic thermal responses for the AlN/W heater with heat pulses of 5 s, 10 s, 15 s, and 20 s, demonstrating the ability to reach temperatures ranging from 700 ˚C to 1000 ˚C. <0001> oriented c-plane sapphire wafers (99.99% purity, MTI Corporation, "c-sapphire") were cut into 1 cm x 1 cm samples as the ZnO deposition substrates.

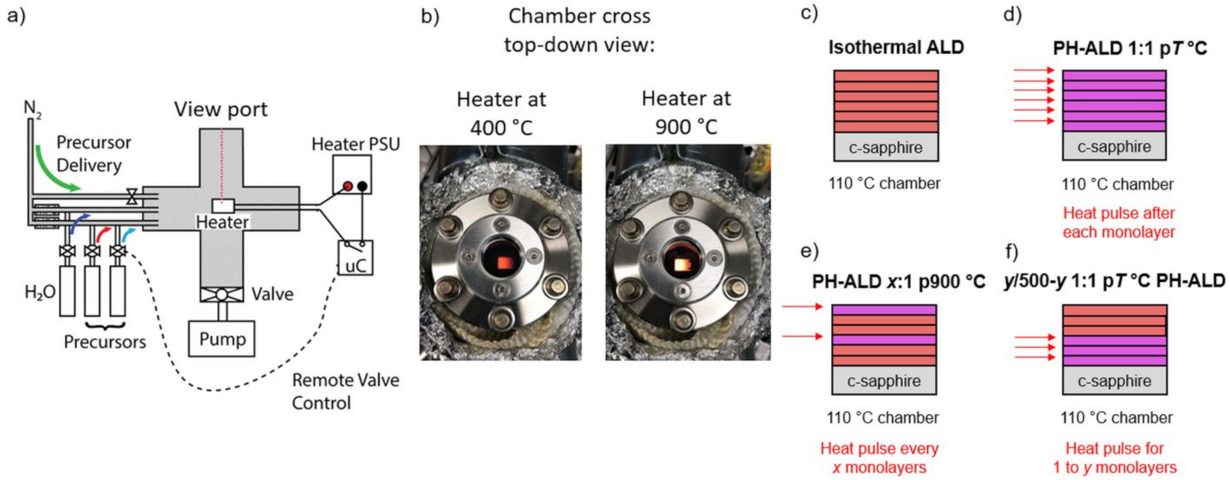

Figure 1. *a) Schematic of PH-ALD chamber. b) Top-down photographs through chamber window looking at heater in (i) mid-heating state and (ii) 900 °C. c,d,e,f) Diagrams of thin film cross-sections schematically representing the c) isothermal ALD process, d) PH-ALD 1:1 pT °C process, e) PH-ALD x:1 p900 °C process, and f) y/500-y 1:1 p900 °C PH-ALD/isothermal ALD templating process. Each horizontal bar represents an ALD cycle; the red arrows indicate when a heat pulse is applied; and the purple layers represent an ALD layer that experiences that heat pulse while on the growth surface.*

Diethylzinc (DEZ, 95% min. purity) from Strem Chemicals (Newburyport, MA, USA) and deionized water were used as the precursor and co-reactant for PH-ALD of ZnO films. Each ALD cycle used a deposition sequence of 0.1 s DEZ / 30 s N_2 purge /

0.1 s H_2O / 30 s N_2 purge, followed by a heat pulse sequence of t_{pulse} / 180 s N_2 purge. For all conditions, 500 ALD cycles were deposited. Growth per cycle (GPC) for all conditions were 0.14-0.18 nm/cycle, consistent with literature values (ESI Figure 2).[4, 32] As presented as schematics in Figure 1c-f, three different deposition series were explored: (1) varying heat pulse temperature (Figure 1d), (2) varying ALD:heat pulse interleave ratio (Figure 1e), and (3) PH-ALD templating (Figure 1f). We denote the PH-ALD conditions as: "PH-ALD x:1 pT ˚C", where x denotes the number of ALD cycles prior to each heat pulse, and T denotes the peak pulse temperature. For the pulse temperature series (Figure 1d), films were grown at pulse temperatures between 400 ˚C and 900 ˚C with one heat pulse for every ALD cycle, PH-ALD 1:1 pT ˚C. For the interleave series (Figure 1e), all heat pulses were performed at 900 ˚C and the ratio of ALD cycles to heat pulses was varied from 1:1 to 5:1, PH-ALD x:1 p900 ˚C. For the templating series (Figure 1f), y PH-ALD cycles at a 900 ˚C pulse temperature and a 1:1 interleave ratio were initially deposited on the substrate, followed by $500 - y$ isothermal ALD cycles at the base chamber temperature (110 °C). The value for y ranged from 1 to 50. Control samples consisted of ALD ZnO films with no pulsed heating grown at 110 °C, referred to as "isothermal ALD" (Figure 1c), and the same ALD ZnO films subjected to a 900 °C PDA in flowing N_2 gas (99.99%+ purity) for one hour, referred to as isothermal ALD + PDA. Due to long deposition times of up to 30 hours, especially for PH-ALD 1:1, most ZnO films were only grown once or twice per condition.

2.2 Characterization

Spectroscopic ellipsometry (alpha-SE, J.A. Woollam) was used to measure film thickness. A GenOsc model with a Tauc-Lorenz oscillator was used as the model for the

ZnO layer with the sapphire substrate. High resolution X-ray diffraction (HR-XRD) was used to characterize the crystallographic orientation of the deposited films. XRD measurements were conducted on a PANalytical Empyrean XRD system using Cu-Ka radation, a BBHD source optic, and a PIXcel 2-dimensional detector. Calibration was conducted by first optimizing the height (Z) and inclination (ω) to the sample. The system was then calibrated to the position of the sapphire crystal by optimizing ω, the normal inclination χ (also referred to as ψ), and finally by 2θ-ω. From this position, 2θ-ω scans (corresponding to θ-2θ geometry in other systems) and ω rocking curves of the *002* ZnO peaks were taken. Off-axis ϕ-scans were then collected for both Al_2O_3 $01\bar{1}8$ and ZnO $10\bar{1}3$ reflections. [17]

Atomic force microscopy (AFM, Bruker Icon) was used to measure surface topography. A n-Si tip (MikroMasch Hq:XSC11/AL) was used with a resonant frequency of 155 kHz, amplitude setpoint between 375-390 mV, and a scan rate of 1 Hz over 1 μm x 1 μm areas. The root mean square (RMS) roughness was calculated using NanoScope Analysis software. Room-temperature photoluminescence (PL) spectroscopy (Horiba Jobin Yvon HR800) with a 325 nm excitation laser was used to measure the optical properties of the films.

3. Results and Discussion

3.1 Crystallography

2θ-ω scans for ZnO films prepared on c-sapphire substrates via (i) isothermal ALD (110 °C), (ii) isothermal ALD + PDA, and (iii) PH-ALD 1:1 p900 ˚C are presented in Figure 2. The isothermal ALD film (i) exhibits 2θ peaks for both the ZnO *002* and *101* reflections, suggesting that the film is random polycrystalline as-deposited. After annealing the as-deposited ALD film to 900 °C for 1 h (ii), ZnO *002* reflection intensity increases significantly but the *101* reflection indicative of a non-epitaxial microstructure remains. In contrast, the PH-ALD film (iii) only exhibits a *002* reflection, suggesting that it is fully textured with its c-axis out-of-plane. Figure 2b plots the ω rocking curves for the *002* ZnO reflections in each of these films to provide some sense of the film's mosaicity. Here, the ω rocking curve FWHM describes the degree of misorientation around the ZnO *002* reflection, where narrower FWHM indicates a smaller distribution of tilts. The PH-ALD film has a rocking curve FWHM of 0.53°. This value is comparable to that grown by other techniques like pulsed electron beam deposition with a FWHM of 0.65°[17] and radio frequency reactive magnetron sputtering with a FWHM of 0.47°,[33] although considerably lower values are reported by PLD (0.048°)[34] and laser MBE (0.004°).[35] However, textured growth in the *c*-plane is a common growth habit for ZnO thin films,[36] and thus, not sufficient to fully confirm its epitaxial in-plane alignment.

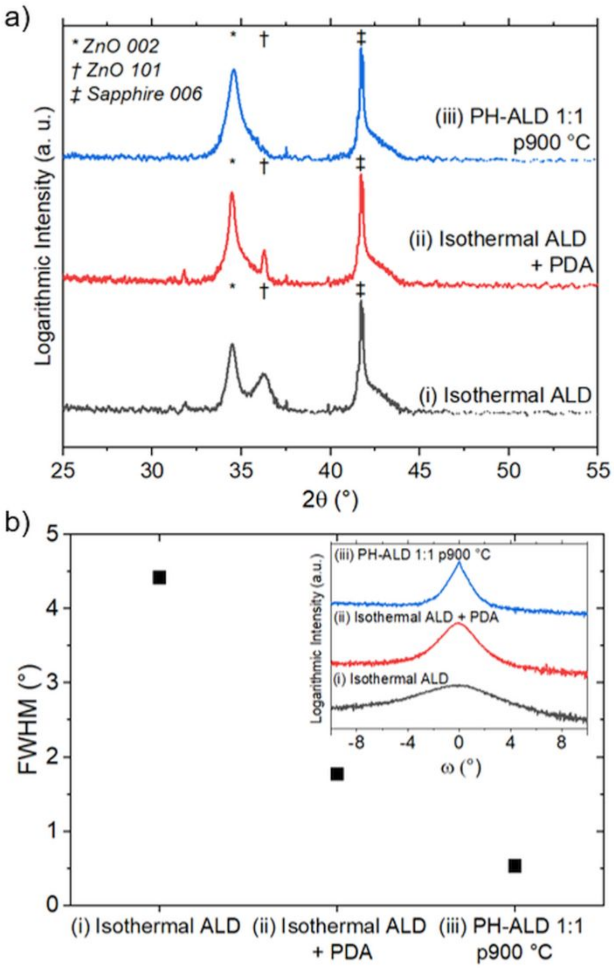

Figure 2. *a) 2θ-ω XRD scans of ZnO films grown on c-sapphire using (i) 110 °C isothermal ALD (bottom), (ii) isothermal ALD + PDA (middle) and (iii) PH-ALD 1:1 p900 ˚C (top). b) Plot of FWHM for the ω-rocking curves of the ZnO 002 peak for films preapared via isothermal ALD, PDA, and PH-ALD; the inset shows the rocking curve traces.*

To fully confirm in-plane epitaxy, Figure 3 presents the off-axis XRD ϕ-scans. For the three conditions presented, (i) isothermal ALD growth, (ii) isothermal ALD with post-deposition N_2 anneal, and (iii) PH-ALD 1:1 p900 °C, the bottom trace is the Al_2O_3 $\mathbf{01\bar{1}8}$ reflection from the sapphire substrate and the top trace is the ZnO $\mathbf{10\bar{1}3}$ reflection. As expected, the bottom traces demonstrate that the rhombohedral sapphire substrate has three off-axis reflections spaced 120° apart from each other at the χ inclination for the Al_2O_3 $01\bar{1}8$ reflection. The ZnO film grown via isothermal ALD (i) shows no reflections in the off-axis ϕ-scan when rocked to the χ inclination for the ZnO $10\bar{1}3$ reflection, suggesting no preferred in-plane orientation as expected for a random poycrystalline material. In contrast, the PH-ALD film (iii) exhibits six well-defined off-axis peaks at this same χ inclination, confirming a preferred in-plane orientation for this crystalline film. Combined with the preferred out-of-plane orientation, we can conclude that these PH-ALD films have grown epitaxially on the c-plane sapphire substrates. Furthermore, the $10\bar{1}3$ ZnO off-axis reflections in Figure 3 are 30° offset from the $01\bar{1}8$ Al_2O_3 reflections of the substrate. This in-plane off-set is the orientation commonly observed for epitaxial growth of wurtizite ZnO on c-plane sapphire with other film growth methods[13, 15] and can be attributed to a ZnO $(0001)[2\bar{1}\bar{1}0]\ //\ Al_2O_3(0001)[1\bar{1}00]$ epitaxial relationship.

Additionally, Figure 3 reveals that the isothermal ALD + PDA film (ii) also shows evidence for a preferred in-plane orientation. While Figure 2 has already indicated that a portion of this film is not textured out-of-plane because the *101* reflection is observed, the off-axis ϕ-scan in Figure 3 (ii) suggests that the portion of the film that is [0001] aligned with the substrate normal includes crystallites that are also aligned in-plane with the sapphire substrate. However, in this PDA film, the in-plane orientation of the $10\bar{1}3$ ZnO reflections have no offset (0°) from the $01\bar{1}8$ reflections of the substrate. This result implies a potentially different mechanism for in-plane templating. A possible explanation is graphoepitaxy from the step-edges of the underlying sapphire substrate. The step-edges of sapphire typically occur along the primary a-axis directions, and similar graphoepitaxy has been reported before for ZnO nanowires.[37] Graphoepitaxy occurs when crystals that want to grow textured out-of-plane become algined in-plane via physical constraints of the substrate.[38] In this case, the sapphire step edges may act as physical constraints that drive in-plane orientation of the ZnO crystals. Upon PDA, these oriented crystals preferentially nucleate and/or further crystallize from these step edges to create this in-plane orientation.

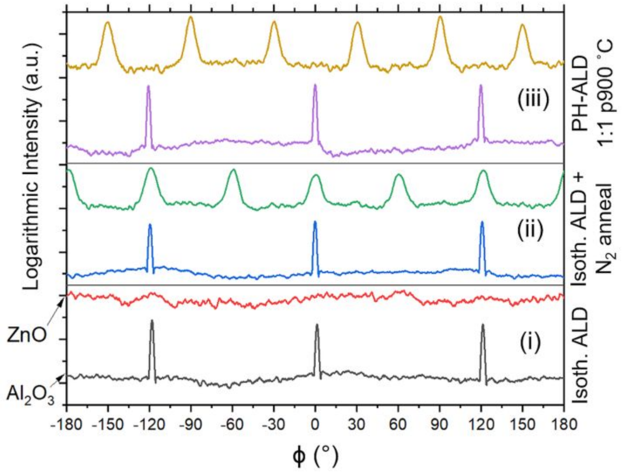

Figure 3. *Off-axis* ϕ*-scans for the* Al_2O_3 $\mathbf{01\bar{1}8}$ *reflection (bottom traces) and ZnO* $\mathbf{10\bar{1}3}$ *reflections (top traces) for (i) isothermal ALD growth conditions, (ii) isothermal ALD with* N_2 *anneal, and (iii) 1:1 p900 ˚C PH-ALD.*

3.2 Varying of PH-ALD Growth Conditions

To investigate the effect of heat pulse temperature, ZnO films were prepared on c-sapphire substrates with maximum pulse temperatures of 400 °C, 500 °C, 600 °C, 700 °C, 800 °C and 900 °C. For these depositions, heat pulses were again applied after every ALD cycle. Figure 4a plots the 2θ-ω diffraction scans (top) and FWHM of the ω-rocking curves (bottom) for each of these films. Here, the control 110 °C isothermal ALD film is plotted as being at a pulse temperature of 110 ˚C. We find that films grown with heat pulses of

400 °C, 600 °C, and 700 °C show both *101* and *002* reflections, indicative of a non-epitaxial polycrystalline microstructure. In contrast, only the *002* reflection is observed for films grown with heat pulses of 800 °C and above. The ω-rocking curves show a generally decreasing FWHM with increasing pulse temperature, ranging from 3.5˚ at 500 ˚C to 0.5˚ at 900 ˚C, suggestive of an increase in crystal quality. With increasing pulse temperature, intra-planar diffusivity increases. We suspect that higher diffusivities cause both the ZnO seed layers to better align with the substrate and for the subsequent ZnO layers to align with the underlying homoepitaxial structure. Futher, in general, this is consistent with literature, where ZnO epilayers grown by other techniques also exhibit better crystal quality at higher growth temperatures.[29]

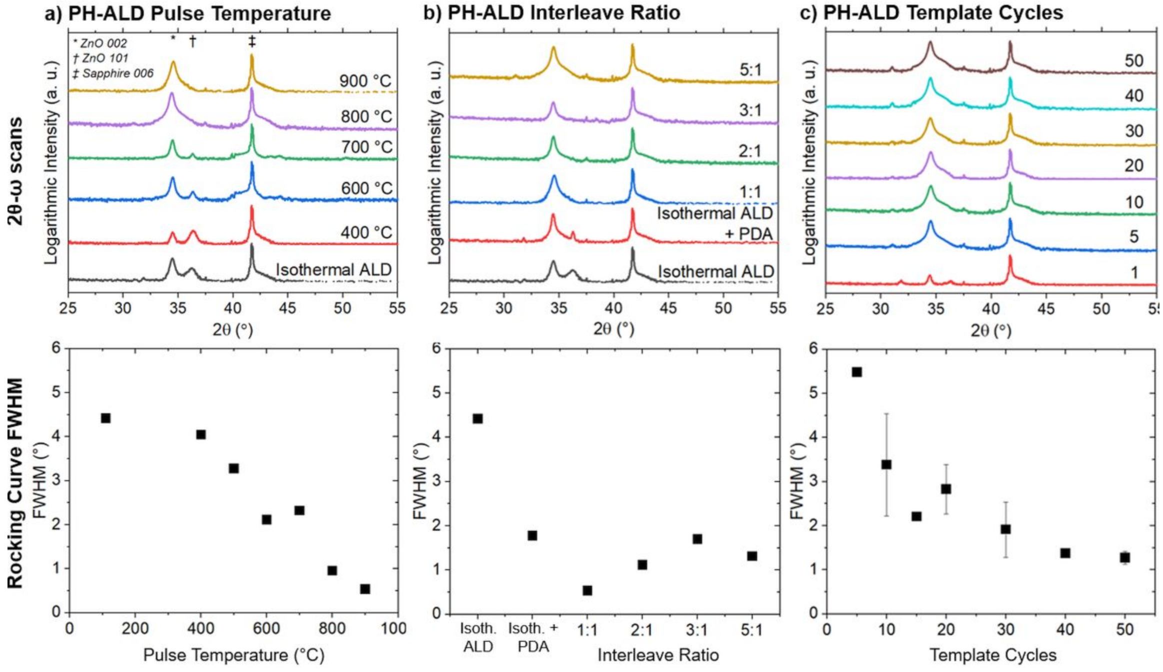

Figure 4. *2θ-ω scans (top) and FWHM of ω rocking curves of the 002 ZnO peak (bottom) for (a) PH-ALD 1:1 films at different pulse temperatures, (b) PH-ALD films of varying [ALD cycles:heat pulse 900 °C] interleave ratios, (c) templated PH-ALD films, with y PH-*

ALD 1:1 p900 °C layers (noted in the annotations on the right) and 500 – y isothermal ALD layers at 110 °C.

Next we investigate the importance of pulse heating after every ALD cycle. Presumably, one advantage to pulse heating after every cycle is that the newly deposited layer is still part of the "surface" such that its diffusion will occur via surface diffusion rather than bulk diffusion. However the true "thickness" of each ALD layer is not always well defined, and we were curious to what extent this layer thickness affected atomic motion and crystal quality. Thus, films were prepared with ratios of ALD-cycles-to-heat-pulses of 1:1, 2:1, 3:1, and 5:1. All heat pulses are to 900 °C. Figure 4b plots the 2θ-ω scans (top) and FWHM of the ω-rocking curves for these films (bottom). Isothermal ALD and PDA films are included in these plots as control references. For all the interleave ratios examined, no non-epitaxial peaks are observed. However, ω-rocking curves have a clear increase in FWHM compared to the 1:1 reference. This decrease in crystalline quality suggests that these thicker layers do reduce atomic mobility (lower diffusivity), likely due to atoms needing to undergo more bulk diffusion than just surface diffusion.

Thirdly, we examine the use of an initial templating layer for "seeding" heteroepitaxial growth. Since low-temperature isothermal homoepitaxy of ALD ZnO with DEZ and water precursors has been demonstrated,[21] thin heteroepitaxial layers grown by PH-ALD on c-sapphire are investigated as templates for subsequent homoepitaxial growth. In all cases 1:1 cycle-to-heating ratios are used with a maximum pulse temperature of 900 °C. "*y*" layers of PH-ALD cycles are grown on the sapphire substrate, followed by *500 – y* isothermal ALD cycles at 110 °C. Here, template cycles ("*y*") of 1, 5, 10, 20, 30, 40, and 50 are investigated. Figure 4c plots the 2θ-ω scans (top) and FWHM of the ω–rocking curves for these films (bottom). For template thicknesses of 5 to 50 PH-ALD layers, only the *002* reflection is present, suggesting that even 5 template cycles is sufficient to promote epitaxial growth. The film with only a single PH-ALD template layer (y = 1) exhibits low-intensity *002* and *101* ZnO XRD reflections, suggesting polycrystallinity and small crystallite size. As shown at the bottom of Figure 4c, the FWHM values for the ω-rocking curves generally decrease with increasing number of template layers. No signal above background could be measured for the 1 cycle PH-ALD templated film. The FWHM decreases from 5.5˚ for the y = 5 template cycles to 1.3˚ for the y = 50 template cycles, indicating significant improvement in the film's epitaxial quality. Here, the improvement appears to plateau above about 40 template cycles and never reaches the FWHM value of about 0.5° observed for growth with 1:1 cycle-to-heating for all 500 layers. Perhaps subsequent homoepitaxial growth at higher temperatures (150 °C to 200 °C) could be used to further improve crystal quality on these template layers.

3.3 Surface Morphology

Figure 5 shows AFM micrographs of the surface morphology for the isothermal ALD, ALD + PDA, and several of the PH-ALD processed films. ESI Figure 3 provides AFM micrograph depth histograms for reference. The isothermal ALD films have an RMS roughness of 1.72 nm, similar to literature values.[39-40] The ALD + PDA films garner a hexagonal morphology with apparently large lateral crystallite sizes of between 100-200 nm and an RMS roughness of 2.09 nm. Note that the edges of these hexagonal features appear to mostly align, suggesting preferrential in-plane alignment as also indicated by the ϕ-scan XRD data in Figure 3 (ii). Note also that each of these large hexagonal features contain much finer structural features (< 10 nm) within them, suggesting a possible substructure to these crystals. In contrast, PH-ALD 1:1 p400 ˚C and PH-ALD 1:1 p900 ˚C films clearly have much smaller overall crystallite sizes of 25 to 35 nm.These films have similar roughness to the PDA film, with the 400 ˚C and 900 °C PH-ALD films having RMS roughnesses of 3.14 nm and 2.19 nm respectively over 1 μm x 1 μm areas. The 50/450 templated film exhibits less well-defined morphological features, like the isothermal ALD morphology, but has evidence of small-grain crystals of similar size and surface roughness to the other PH-ALD films. The difference in morphology between the PDA and PH-ALD films further indicates the difference in their crystallization processes.

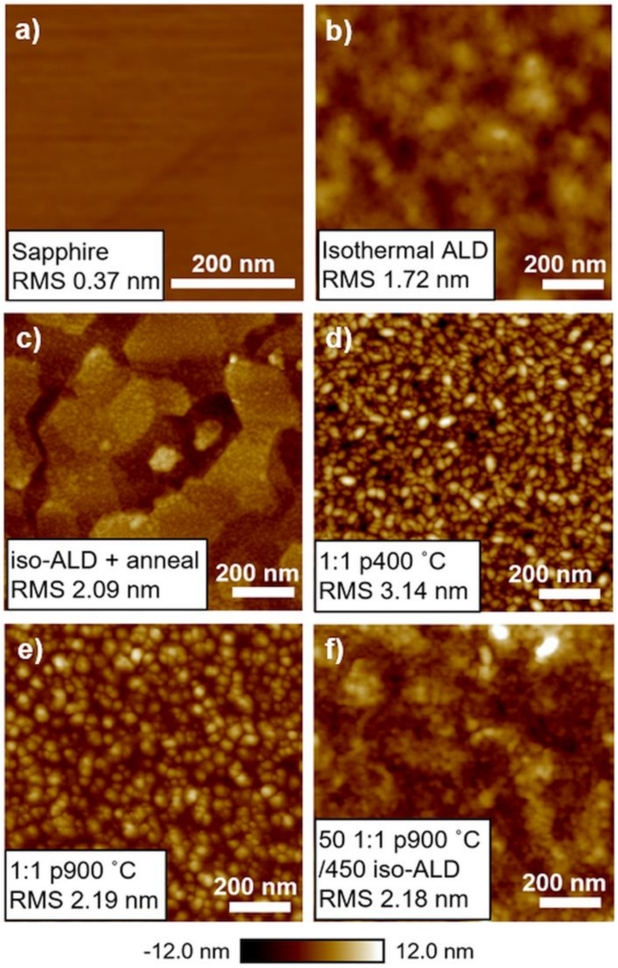

Figure 5. *AFM images of surface morphology for: a) bare c-sapphire substrate, b) an isothermal ALD ZnO film grown at 110 °C on c-sapphire, c) isothermally grown ALD ZnO film grown on c-sapphire and then PDA at 900 °C in* N_2 *for 1 h, d) PH-ALD 1:1 p400 ˚C ZnO film grown on c-sapphire, e) PH-ALD 1:1 p900 ˚C ZnO film grown on c-sapphire, and f) 50/450 PH-ALD templated ZnO film grown on c-sapphire. Images are from a 1 µm x 1 µm scan, with RMS roughness values calculated on a frame average basis and shown for each underneath the image.*

3.4 Optical Properties

Room temperature photoluminescence was performed on these ZnO films to determine how the differences in crystalline structure achieved with varying PH-ALD process conditions affect this photoelectronic property. Prior works have demonstrated that epitaxial ZnO films grown at higher temperatures with improved crystalline quality show improved PL performance.[41-42] Figure 6 plots the room temperature photoluminescence spectra for PH-ALD films with varying cycle-to-heating interleaving ratios. All films exhibit a single emission peak centered at 3.30 eV. This peak corresponds to band-edge emission of ZnO.[28] The intensity of this emission peak increases with decreasing interleave ratios, further confirming the reported improvement in crystalline quality from the ω-rocking curves and indicating that heat pulses decrease residual impurities and dislocations. The emission intensity from the PH-ALD 1:1 p900 °C epitaxial film exceeds the PL emission intensity of the isothermal ALD polycrystalline film by more than an order of magnitude. The isothermal ZnO film that underwent PDA has an intermediate to high PL intensity, but its emission peak energy is offset from the PH-ALD films at 3.28 eV. This shift in the emission energy is possibly due to a difference in crystallite size or strain state and is similar to the peak emission energy of the isothermal ALD film. The FWHM values of the PL emission for all ZnO films are approximately 0.1 eV, which is consistent with what can be observed for room temperature PL of ZnO,[43-45] although far lower values have been reported by laser MBE.[35] While more sophisticated measurements would be needed to identify the exact differences observed here for varying growth conditions, including low temperature PL measurements, these room temperature PL results do follow the generally expected trend of higher PL emission with improved crystal quality.

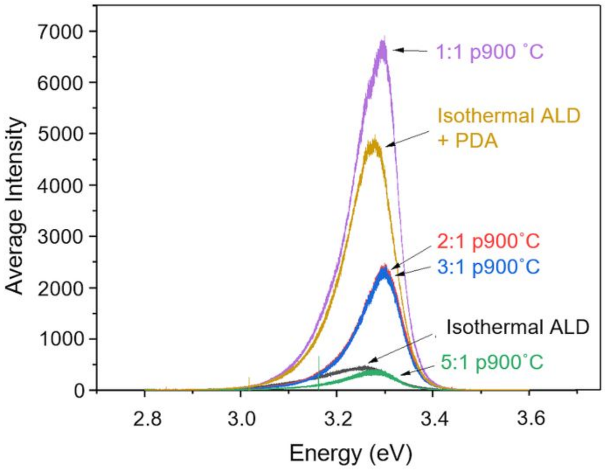

Figure 6. *Room-temperature photoluminescence spectra for isothermal ALD, isothermal ALD + PDA, and interleaved PH-ALD ZnO films grown on c-sapphire.*

4. Conclusions

PH-ALD was used to grow heteroepitaxial ZnO thin films on c-plane sapphire substrates using a high-power resistive heating stage. Pulse temperatures above 800 °C were shown to be necessary to eliminate non-epitaxial, polycrystalline film deposition. In general, higher pulse temperatures and more frequent pulses improved epitaxial quality, although reasonable epitaxy could be achieve with just 5 PH-ALD template cycles. While PDA of low-temperature isothermal (110 °C) ZnO films did achieve some in-plane alignment to the ZnO crystals, films never became fully epitaxial and interestingly the in-plane orientation with the substrate was 30° offset from the PH-ALD films, suggesting a different crystallization templating mechanism, possibly graphoepitaxy. Morphologically, the PDA films had what appeared to be larger crystallites than the PH-ALD but also a potentially finer substructure. Photoluminescence emission also generally increased with the crystalline quality of the PH-ALD ZnO films. These results demonstrate the utitlity of

PH-ALD as a means to impose epitaxial templating and manipulate crystallinity in an ALD process that is otherwise constrained to low temperatures due to the use of temperature-sensitive metalorganic precursors. Further advances to this process technology will likely require better understanding how high-quality template layers can be grown such that process times can be kept shorter while still retaining good crystalline quality throughout the entire film.

5. Author Contributions

B.D.P. contributed the initial concept, reactor design and material preparation, crystallography, and initial manuscript. J.P.W contributed additional material preparation, characterization, and text revisions. S.A.G. contributed characterization and text revisions. M.D.L contributed the initial concept, research support, and text revisions.

6. Conflicts of Interest

There are no conflicts of interest to declare.

7. Acknowledgements

B.D.P. acknowledges financial support from the National Defense Science and Engineering Graduate (NDSEG) fellowship program. J.P.W acknowledges support from the National Science Foundation Graduate Research Fellowship Program under Grant No. DGE-1650044. S.A.G acknowledges financial support from a Link Foundation Energy Fellowship. A portion of this work was performed at the Georgia Tech Institute for Electronics and Nanotechnology, a member of the National Nanotechnology Coordinated Infrastructure (NNCI), which is supported by the National Science

Foundation (ECCS-2025462). B.D.P. thanks S. Graham and N. Hines for assistance with PL measurements and D. Tavakoli for assistance with XRD measurements.

REFERENCES

1. Johnson, R. W.; Hultqvist, A.; Bent, S. F., A Brief Review of Atomic Layer Deposition: From Fundamentals to Applications. **2014**, *17*, 236-246.
2. Miikkulainen, V.; Leskelä, M.; Ritala, M.; Puurunen, R. L., Crystallinity of Inorganic Films Grown by Atomic Layer Deposition: Overview and General Trends. *Journal of Applied Physics* **2013**, *113*, 021301.
3. George, S. M., Atomic Layer Deposition: An Overview. *Chemical Reviews* **2010**, *110*, 111-131.
4. Conley, J. F.; Ono, Y.; Tweet, D. J., Densification and Improved Electrical Properties of Pulse-Deposited Films Via in Situ Modulated Temperature Annealing. *Applied Physics Letters* **2004**, *84*, 1913-1915.
5. Conley Jr, J. F.; Ono, Y.; Stecker, G. M., Modulated Temperature Method of Atomic Layer Deposition (Ald) of High Dielectric Constant Films. Google Patents: 2008.
6. Nabatame, T., et al. In *Design and Proof of High Quality Hfalo/Sub X/ Film Formation for Moscaps and Nmosfets through Layer-by-Layer Deposition and Annealing Process*, 2003 Symposium on VLSI Technology. Digest of Technical Papers (IEEE Cat. No.03CH37407), 10-12 June 2003; 2003; pp 25-26.
7. Langston, M. C.; Dasgupta, N. P.; Jung, H. J.; Logar, M.; Huang, Y.; Sinclair, R.; Prinz, F. B., In Situ Cycle-by-Cycle Flash Annealing of Atomic Layer Deposited Materials. *J. Phys. Chem. C* **2012**, *116*, 24177-24183.
8. Henke, T.; Knaut, M.; Hossbach, C.; Geidel, M.; Albert, M.; Bartha, J. W., Growth of Aluminum Oxide Thin Films with Enhanced Film Density by the Integration of in Situ Flash Annealing into Low-Temperature Atomic Layer Deposition. *Surface and Coatings Technology* **2017**, *309*, 600-608.
9. Wang, Z. L., From Nanogenerators to Piezotronics—a Decade-Long Study of Zno Nanostructures. *MRS Bulletin* **2012**, *37*, 814-827.
10. Law, M.; Greene, L. E.; Johnson, J. C.; Saykally, R.; Yang, P., Nanowire Dye-Sensitized Solar Cells. *Nature Materials* **2005**, *4*, 455-459.
11. Huang, M. H.; Mao, S.; Feick, H.; Yan, H.; Wu, Y.; Kind, H.; Weber, E.; Russo, R.; Yang, P., Room-Temperature Ultraviolet Nanowire Nanolasers. *Science* **2001**, *292*, 1897.
12. Srikant, V.; Sergo, V.; Clarke, D. R., Epitaxial Aluminum-Doped Zinc Oxide Thin Films on Sapphire: I, Effect of Substrate Orientation. *Journal of the American Ceramic Society* **1995**, *78*, 1931-1934.
13. Chen, Y.; Tuan, N. T.; Segawa, Y.; Ko, H.-j.; Hong, S.-k.; Yao, T., Stimulated Emission and Optical Gain in Zno Epilayers Grown by Plasma-Assisted Molecular-Beam Epitaxy with Buffers. *Applied Physics Letters* **2001**, *78*, 1469-1471.

14. Hiroyuki, K.; Michihiro, S.; Kazuhiro, M.; Takafumi, Y., Effect of O/Zn Flux Ratio on Crystalline Quality of Zno Films Grown by Plasma-Assisted Molecular Beam Epitaxy. *Japanese Journal of Applied Physics* **2003**, *42*, 2241.
15. Chen, Y.; Bagnall, D. M.; Koh, H.-j.; Park, K.-t.; Hiraga, K.; Zhu, Z.; Yao, T., Plasma Assisted Molecular Beam Epitaxy of Zno on C -Plane Sapphire: Growth and Characterization. *Journal of Applied Physics* **1998**, *84*, 3912-3918.
16. Triboulet, R.; Perrière, J., Epitaxial Growth of Zno Films. *Progress in Crystal Growth and Characterization of Materials* **2003**, *47*, 65-138.
17. Tricot, S.; Nistor, M.; Millon, E.; Boulmer-Leborgne, C.; Mandache, N. B.; Perrière, J.; Seiler, W., Epitaxial Zno Thin Films Grown by Pulsed Electron Beam Deposition. *Surface Science* **2010**, *604*, 2024-2030.
18. Ogata, K.; Maejima, K.; Fujita, S.; Fujita, S., Growth Mode Control of Zno toward Nanorod Structures or High-Quality Layered Structures by Metal-Organic Vapor Phase Epitaxy. *Journal of Crystal Growth* **2003**, *248*, 25-30.
19. Karpina, V. A., et al., Zinc Oxide – Analogue of Gan with New Perspective Possibilities. *Crystal Research and Technology* **2004**, *39*, 980-992.
20. Bielinski, A. R.; Kazyak, E.; Schlepütz, C. M.; Jung, H. J.; Wood, K. N.; Dasgupta, N. P., Hierarchical Zno Nanowire Growth with Tunable Orientations on Versatile Substrates Using Atomic Layer Deposition Seeding. *Chemistry of Materials* **2015**, *27*, 4799-4807.
21. Elam, D.; Ortega, E.; Nemashkalo, A.; Strzhemechny, Y.; Ayon, A.; Ponce, A.; Chabanov, A. A., Low-Defect-Density Zno Homoepitaxial Films Grown by Low-Temperature Ald. *Applied Physics Letters* **2021**, *119*, 142101.
22. Kukushkin, S. A.; Osipov, A. V.; Romanychev, A. I., Epitaxial Growth of Zinc Oxide by the Method of Atomic Layer Deposition on Sic/Si Substrates. *Physics of the Solid State* **2016**, *58*, 1448-1452.
23. Särkijärvi, S.; Sintonen, S.; Tuomisto, F.; Bosund, M.; Suihkonen, S.; Lipsanen, H., Effect of Growth Temperature on the Epitaxial Growth of Zno on Gan by Ald. *Journal of Crystal Growth* **2014**, *398*, 18-22.
24. Kopalko, K.; Godlewski, M.; Domagala, J. Z.; Lusakowska, E.; Minikayev, R.; Paszkowicz, W.; Szczerbakow, A., Monocrystalline Zno Films on Gan/Al2o3 by Atomic Layer Epitaxy in Gas Flow. *Chemistry of Materials* **2004**, *16*, 1447-1450.
25. Kopalko, K.; Wójcik, A.; Godlewski, M.; Łusakowska, E.; Paszkowicz, W.; Domagała, J. Z.; Godlewski, M. M.; Szczerbakow, A.; Świątek, K.; Dybko, K., Growth by Atomic Layer Epitaxy and Characterization of Thin Films of Zno. *physica status solidi (c)* **2005**, *2*, 1125-1130.
26. Baji, Z.; Lábadi, Z.; Molnár, G.; Pécz, B.; Vad, K.; Horváth, Z. E.; Szabó, P.; Nagata, T.; Volk, J., Highly Conductive Epitaxial Zno Layers Deposited by Atomic Layer Deposition. *Thin Solid Films* **2014**, *562*, 485-489.
27. Kaiya, K.; Yoshii, N.; Takahashi, N.; Nakamura, T., Atmospheric Pressure Atomic Layer Epitaxy of Zno on a Sapphire (0001) Substrate by Alternate Reaction of Zncl2 and O2. *Journal of Materials Science Letters* **2000**, *19*, 2089-2090.
28. Kaiya, K.; Yoshii, N.; Omichi, K.; Takahashi, N.; Nakamura, T.; Okamoto, S.; Yamamoto, H., Atmospheric Pressure Atomic Layer Epitaxy of Zno Using a Chloride Source. *Chemistry of Materials* **2001**, *13*, 1952-1956.

29. Özgür, Ü.; Alivov, Y. I.; Liu, C.; Teke, A.; Reshchikov, M. A.; Doğan, S.; Avrutin, V.; Cho, S. J.; Morkoç, H., A Comprehensive Review of Zno Materials and Devices. *Journal of Applied Physics* **2005**, *98*, 041301.
30. Yang, S.; Lin, B.-H.; Liu, W.-R.; Lin, J.-H.; Chang, C.-S.; Hsu, C.-H.; Hsieh, W.-F., Structural Characteristics and Annealing Effect of Zno Epitaxial Films Grown by Atomic Layer Deposition. *Crystal growth & design* **2009**, *9*, 5184-5189.
31. Piercy, B. D.; Losego, M. D., Tree-Based Control Software for Multilevel Sequencing in Thin Film Deposition Applications. *Journal of Vacuum Science & Technology B* **2015**, *33*, 043201.
32. Langston, M. C.; Dasgupta, N. P.; Jung, H. J.; Logar, M.; Huang, Y.; Sinclair, R.; Prinz, F. B., In Situ Cycle-by-Cycle Flash Annealing of Atomic Layer Deposited Materials. *The Journal of Physical Chemistry C* **2012**, *116*, 24177-24183.
33. Liu, H.; Zeng, F.; Lin, Y.; Wang, G.; Pan, F., Correlation of Oxygen Vacancy Variations to Band Gap Changes in Epitaxial Zno Thin Films. *Applied Physics Letters* **2013**, *102*, 181908.
34. Liu, W.-R.; Hsieh, W.-F.; Hsu, C.-H.; Liang, K. S.; Chien, F.-S., Threading Dislocations in Domain-Matching Epitaxial Films of Zno. *Journal of Applied Crystallography* **2007**, *40*, 924-930.
35. Ohkubo, I.; Matsumoto, Y.; Ohtomo, A.; Ohnishi, T.; Tsukazaki, A.; Lippmaa, M.; Koinuma, H.; Kawasaki, M., Investigation of Zno/Sapphire Interface and Formation of Zno Nanocrystalline by Laser Mbe. *Applied surface science* **2000**, *159*, 514-519.
36. Fujimura, N.; Nishihara, T.; Goto, S.; Xu, J.; Ito, T., Control of Preferred Orientation for Znox Films: Control of Self-Texture. *Journal of Crystal Growth* **1993**, *130*, 269-279.
37. Tsivion, D.; Schvartzman, M.; Popovitz-Biro, R.; Joselevich, E., Guided Growth of Horizontal Zno Nanowires with Controlled Orientations on Flat and Faceted Sapphire Surfaces. *ACS Nano* **2012**, *6*, 6433-6445.
38. Givargizov, E. I., Graphoepitaxy as an Approach to Oriented Crystallization on Amorphous Substrates. *Journal of Crystal Growth* **2008**, *310*, 1686-1690.
39. Elam, J.; Sechrist, Z.; George, S., Zno/Al2o3 Nanolaminates Fabricated by Atomic Layer Deposition: Growth and Surface Roughness Measurements. *Thin Solid Films* **2002**, *414*, 43-55.
40. Banerjee, P.; Lee, W.-J.; Bae, K.-R.; Lee, S. B.; Rubloff, G. W., Structural, Electrical, and Optical Properties of Atomic Layer Deposition Al-Doped Zno Films. *Journal of Applied Physics* **2010**, *108*, 043504.
41. Ku, C.-S.; Lee, H.-Y.; Huang, J.-M.; Lin, C.-M., Epitaxial Growth of M-Plane Zno Thin Films on (1010) Sapphire Substrate by Atomic Layer Deposition with Interrupted Flow. *Crystal growth & design* **2010**, *10*, 1460-1463.
42. Kumar, A.; Jeedigunta, S.; Tarasov, I.; Ostapenko, S., Photoluminescence Studies of Epitaxial Zno Thin Films on Si (1 0 0) Substrates by Pulsed Laser Deposition, Azo J. *Mater* **2010**, *6*, 1-10.
43. Liu, W.-R.; Li, Y.-H.; Hsieh, W.; Hsu, C.-H.; Lee, W.; Lee, Y.; Hong, M.; Kwo, J., Domain Matching Epitaxial Growth of High-Quality Zno Film Using a Y2o3 Buffer Layer on Si (111). *Crystal Growth and Design* **2009**, *9*, 239-242.

44. Huang, M. H.; Wu, Y.; Feick, H.; Tran, N.; Weber, E.; Yang, P., Catalytic Growth of Zinc Oxide Nanowires by Vapor Transport. *Advanced Materials* **2001**, *13*, 113-116.

45. Yang, S.; Kuo, C.; Liu, W.-R.; Lin, B.; Hsu, H.-C.; Hsu, C.-H.; Hsieh, W., Photoluminescence Associated with Basal Stacking Faults in C-Plane Zno Epitaxial Film Grown by Atomic Layer Deposition. *Applied Physics Letters* **2012**, *100*, 101907.